**WUJNS**
Wuhan University Journal of Natural Sciences

Vol.10 No.3 2005 529-533

**Article ID:** 1007-1202(2005)03-0529-05

# Silicon-Based Grid Structure Photodiode with Selective UV Enhancement

**WANG Ying**[1], **CHEN Bing-ruo**[1, 2†], **LIU Yu-ping**[1]

1. School of Physics and Technology, Wuhan University, Wuhan 430072, Hubei, China;
2. State Key Laboratory of Transducer Technology, Chinese Academy of Sciences, Shanghai 200050, China

---

**Abstract:** Aiming at boosting the low ultraviolet (UV) responsivity induced by the negative impact of the surface 'dead layer' in silicon-based conventional photodiode (CPD), Si photodiodes with five different structures, including both the novel grid structure photodiode (GSPD) and CPD, have been manufactured using thermal diffusion process and tested. The results show that the UV responsivity around 365 nm of GSPD could be as high as 6 times that of CPD, while the high visible (VIS) responsivity is sharply suppressed by the employment of grid shaped junction (GSJ) in the GSPD, which has realized the expectation of selective UV enhancement with prospect for application.

**Key words:** responsivity; selective ultraviolet enhancement; grid-shaped junction; silicon ultraviolet photodiode

**CLC number:** O 472$^+$.1

## 0 Introduction

UV photodetectors exhibit more and more significance in both defense related and civilian applications, e. g., in missile plume detection[1], flame monitoring[2,3] and measurement of UV irradiation of people[4,5], *et al.* Therefore, diverse technologies and materials have been employed to obtain high performance UV detectors, they are generally divided into two categories, i. e., vacuum devices with high intrinsic selectivity, sensitivity and gain, but fragile and bulky, and the other type, solid state semiconductor devices with high efficiency, low dark current, lightweight and good integrability with signal processing IC. As subspecies of the latter type, UV photodiodes based on compound semiconductors such as AlGaN, GaN, ZnSe and SiCN, *et al*, have shown higher impedance and better capability for high frequency operation than photoconductive cells and higher sensitivity and selectivity and shorter response time than the Si-based photodiodes[6-10], however, in case of the monolithical integration of photodiodes, especially their array, with the associated circuits upon a single silicon substrate with high performance and reliability, Si devices are still the prior options in view of both the compatibility of its fabrication process and its cost effectiveness.

The UV responsivity of CPD fabricated using thermal diffusion process is substantially limited by the surface and bulk property of the substrate [11], until recently, employment of devices with ultra shallow junction, suppression of surface recombination and introduction of built-in electric field driving the carriers to the active pn$^-$ junction are the three frequently adopted approaches to lift the UV responsivity[1]. In this paper, a novel GSPD with unique geometry is proposed and realized. A detailed discussion is presented about the

---

**Received date:** 2004-10-28

**Foundation item:** Supported by the Foundation of State key Laboratory of Transducer Technology of Shanghai (SKt 0401)

**Biography:** WANG Ying (1981-), male, Master candidate, research direction: semiconductor devices, OLED and related circuits, E-mail: wy810418@21cn. com. cn

† To whom correspondence should be addressed. E-mail: brchen@whu. edu. cn

mechanism of its operation and merits of this device.

## 1 Experimental

### 1.1 Some Crucial Factors Influencing the UV Responsivity

For Si photodiodes operating in the spectral range of 200-400 nm, most of the UV photo-generated carriers (PGC) are excited in the less than 100 nm thick surface layer due to the high absorption coefficient of $10^6$-$10^5$ cm$^{-1}$[12,13], the doping density $N_s$ of this surface area is generally limited to $10^{19}$-$10^{20}$ cm$^{-3}$ by the constraint of solid solubility of boron in silicon, which leads to the following unfavorable effects:

1) As the surface doping density exceeds $10^{20}$ cm$^{-3}$, the diffusion length of minority carriers shorter than 1 $\mu$m leads to the failing collection of PGC by the active junction of CPD.

2) For boron diffusion, The "band gap narrowing" effect induced by high surface doping density will incur a unfavorable drift field within a tens-of-nanometers-thick surface 'dead layer'[14,15], driving the PGC drift to the incident surface rather than the active junction, thus decreasing the internal quantum efficiency (IQE), which naturally reduces the UV responsivity.

3) Auger recombination in this region degrades the lifetime of PGC, further reducing the diffusion length, conclusively bringing down the UV responsivity.

### 1.2 Design of the Photodiodes

1) The operating principle of GSPD

This work is done because we believe the novel structure of GSPD would boost UV responsivity while suppressing the unwanted VIS responsivity. For CPD, the negative built-in electric field induced by the abnormal distribution of boron doping density within the 'dead layer' drives most of the UV PGC away from the active pn$^-$ junction, and then these PGC are annihilated by recombination, making the UV responsivity degraded significantly. While for GSPD shown in Fig. 1, there is no 'dead layer' in the n$^-$ active region, thus, when the region between two adjacent ($p^+n^-$) GSJ is fully depleted by applying a proper reverse bias between the cathode and the anode, most UV PGC could be laterally collected by the wall side of GSJ, yielding UV responsivity much higher than that of CPD.

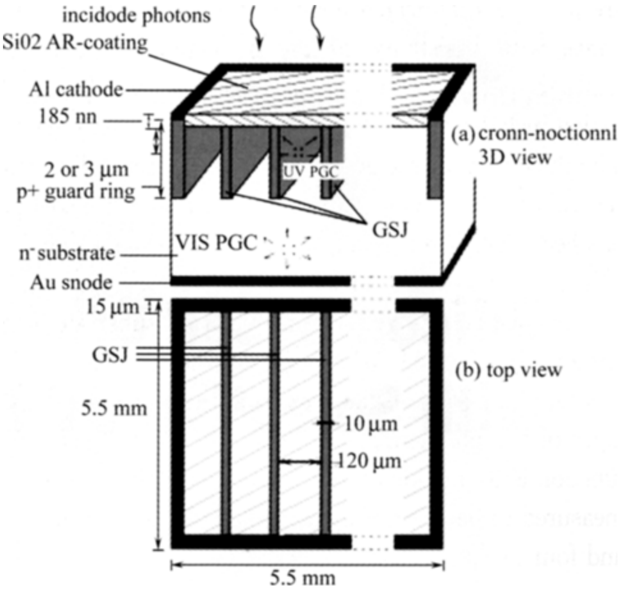

**Fig. 1 Schematic of GSPD**

Only by making the depth of GSJ larger than UV penetration depth, the UV PGC can be excited between every two adjacent GSJ be collected by the sidewall GSJ and form photocurrent as shown in the Fig. 1(a). Nevertheless, as the penetration depth of VIS photon is larger than that of UV photon, most of the VIS PGC are therefore excited outside the active region of GSJ, which suppresses the VIS responsivity, this is the key to achieving the selective UV enhancement. Taking into account all the above, the depths of GSJ are designed to be 2 and 3 $\mu$m respectively.

The distance between the adjacent GSJ and the width of GSJ has been optimized to maximize IQE based on the following analysis: The doping density of the n$^-$ type substrate is about $5.0\times10^{13}$ cm$^{-3}$, the mobility of hole $\mu_p=500$ cm$^2\cdot$V$^{-1}\cdot$s$^{-1}$[16] at room temperature, its diffusion coefficient $D_P=13$ cm$^2\cdot$s$^{-1}$[16], so the surface diffusion length $L$ is deduced as 250 $\mu$m, nevertheless, the accurate value of the incident-surface-layer-quality dependent recombination lifetime $\tau$ of hole is not available, referring to some literatures[17-19], a best value and a worst value are taken as $\tau_1=1\,300\times10^{-7}$ s, $\tau_2=1.0\times10^{-7}$ s, respectively, then the best value and worst value $L_1=411$ $\mu$m, $L_2=11.4$ $\mu$m are deduced respectively. Based on the above analysis, the distance $D$ between the GSJ, the number and width $W$ of GSJ are defined as 120, 42, 10 $\mu$m respectively. For this configuration of GSPD, the key to improving the performance of UV photodiode is that the ratio of the area without 'dead layer' to the whole area is about 92%.

2) The structure of GSPD

As illustrated in Fig. 1, both the guard ring and GSJ are $p^+$ layers fabricated upon a ⟨1 1 1⟩ $n^-$ type Si substrate with resistivity of approximately 100-120 cm, while the rest area is original $n^-$ substrate. The active region includes the GSJ and the region between the GSJ. The dimension of the active region is 5. 5 mm×5. 5 mm, the 185nm thick $SiO_2$ antireflection coating(AR-coating) has been designed specially for 365 nm incident light.

3) The structure of CPD

As shown in Fig. 2, the active area, substrate material and thickness of AR-coating are the same as those of GSPD, the rest of surface area is a p layer except the $p^+$ layer of the guard ring. The depth of $p^+ n^-$ guard ring junction is 3 or 2 μm, while the depth of the p layer was measured to be 320 nm by combined usage of anodization and four probe method.

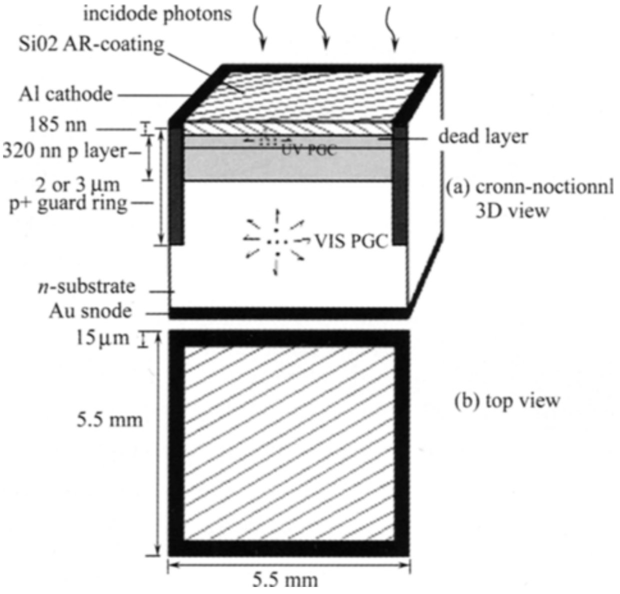

Fig. 2 Schematic of CPD

## 1.3 Fabrication Process

All the above devices were fabricated by thermal diffusion process. The $n^-$ type Si substrate is doped with boron to form $p^+$ and p layer with different doping density. To reduce the surface sheet resistance, the surface impurity density and the depths of the GSJ are controlled to be about $10^{19}$ $cm^{-3}$, 2 μm and 3 μm respectively; while for CPD, the surface impurity density of p layer was measured to be about $10^{17}$-$10^{18}$ $cm^{-3}$ by combined usage of anodization and four probe method.

# 2 Results and Discussion

## 2.1 Discussion on the Experimental Results

To make a comparison of the UV response sensitive factors, devices with five different geometric parameters have been fabricated, namely: ① GSPD with 2 μm GSJ depth; ② GSPD with 3 μm GSJ depth; ③ CPD shown in Fig. 2; ④ combined structure of ①&③; ⑤ combined structure of ②&③. To make it brief, let ①、②、③、④、⑤represent the five devices respectively in the following discussion.

1)As shown in Fig. 3, the responsivity of GSPD is about 3. 5 times larger than that of CPD at 365 nm under low reverse bias condition, however, these two responsivities tend to be equal when $\lambda$ increases to about 410 nm, as $\lambda$ becomes longer into the VIS range, the ratio of the former to the latter responsivity decreases to 0. 5-0. 6 and finally retains constant.

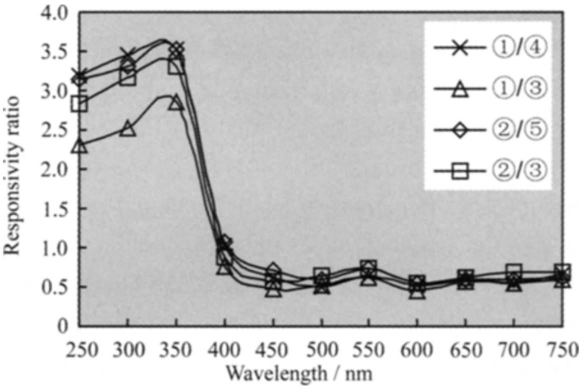

Fig. 3 Responsivity ratio versus wavelength at−1V

The above results have confirmed the selective UV enhancement effect stemming from the unique structure of GSPD as analyzed in section 1. 2, thus the critical impact of the surface 'dead layer' upon the UV responsivity has been testified.

2) As shown in Fig. 4, the responsivity ratio of GSPD to CPD at 365 nm increases almost linearly with reverse bias, until the bias reaches a threshold value when the ratio stops increasing at a bias-independent maximum value, about 4-6, this threshold voltage is about −6-−7 V. This is traceable to the fact that: for GSPD, the proportional increase of the GSJ depletion region with increasing reverse bias leads to a more effective sidewall collection of UV PGC. Contrarily for CPD suffering from the recombination effect within the surface 'dead layer', the increase of its UV responsivity induced by its increased-bias-induced depletion region expanding is relatively weaker. when the expanded depletion region is bulky enough to collect all the UV PGC as the reverse bias reaches the above threshold voltage, the increment of the above ratio approaches to zero. This result is in

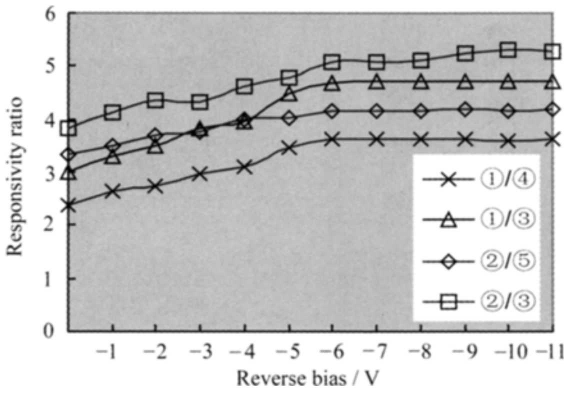

**Fig. 4 Responsivity ratio versus reverse bias at 365 nm**

good agreement with the qualitative analysis and prediction based on semiconductor theory.

As shown in Fig. 5, the responsivity ratio of GSPD to CPD at 700 nm is about 0. 4-0. 6 under low reverse bias less than −1 V, which means the 700 nm responsivity of GSPD is much smaller than that of CPD. this is due to the combined effect of the relatively larger depletion region of CPD than that of GSPD under low bias condition and the larger penetration depth of 700 nm light, about 5 μm[16], than the depth of GSJ, which makes most of the 700 nm PGC be collected more effectively by the $pn^-$ shallow junction of CPD than by the GSJ, so the 700 nm responsivity of GSPD is relatively weaker compared to the CPD counterpart. Nevertheless, the responsivity ratio increases to 0. 9-0. 95 and then retains constant as the bias increases to a threshold value, this can be explained by the fact that the depletion region gradually expands with increasing reverse bias, under the assumption of 'depletion approximation', the width of the depletion region in the $n^-$ region of GSPD is deduced to be 4. 4 and 4. 8 μm for ②、③ respectively at zero bias, which are too small for GSPD to collect the 700nm PGC effectively, while at −5 V, the two values are 12. 2 μm and 13. 2 μm respectively, which is comparable to the penetration depth of 700 nm light, making the 700 nm responsivities of GSPD and CPD tend to be equal. Base on the principle described in the above paragraph, there also exist a wavelength-dependent threshold voltage much larger than the one in the above paragraph, which is about −10-−11 V, this is probably due to the relatively larger penetration depth of 700 nm than that of 365 nm light.

3) The absolute responsivity versus wavelength curves of both ①type GSPD and ③type CPD under −1 V reverse bias are shown in Fig. 6, even though the curve of GSPD is not so perfect that its UV responsivity overshoot its VIS counterpart, it is still very cheering to see that the poor UV responsivity of CPD is greatly enhanced by the GSPD, while the undesirable high VIS counterpart has been successfully suppressed.

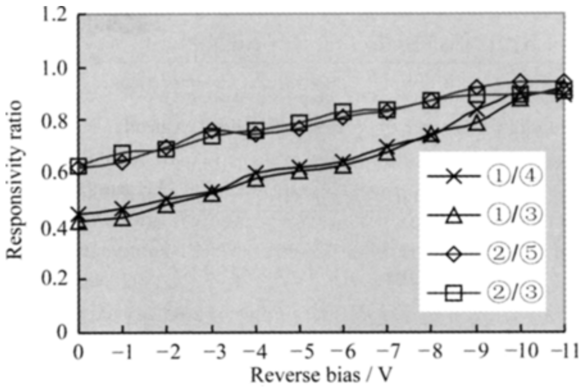

**Fig. 5 Responsivity ratio versus reverse bias at 700 nm**

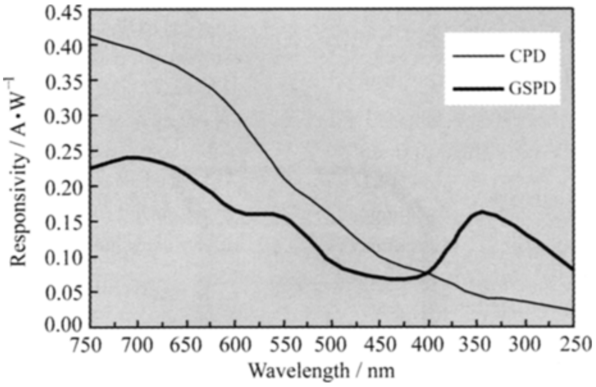

**Fig. 6 Responsivity versus wavelength of ②GSPD and ③ CPD at −1 V**

## 2.2 Responsivity Curves

The responsivity of the five different devices was measured under same condition, the responsivity ratios of ① to ④, ① to ③, ② to ⑤ and ② to ③ were given under the same incident power density 8. 6 $\mu W \cdot cm^{-2}$.

## 2.3 Dark Current

The dark current of all the fabricated devices exhibits the same order of magnitude at −5 V, the typical value is less than 0. 1 nA。

The photodiodes were illuminated by mercury lamp with line spectrum through a color filter (from Andover Corporation). The illumination power was measured with OMM-6810B photo dynamometer. Photocurrent was measured with DT830 digital circuit tester produced by KEITHLEY. The UV responsivity of ① and ② is about 0. 16 $A \cdot W^{-1}$ at 365 nm and about 0. 08 $A \cdot W^{-1}$ at 254 nm ( another typical UV wavelength) at −1 V.

## 3 Conclusion

The novel GSPD with two different GSJ depths based on $n^-$ silicon substrate was fabricated together with CPD. Their UV responsivities were compared. The results imply that, in photovoltaic operation, and the UV responsivity of GSPD is more than 3 times larger than that of CPD, while in the VIS range, the responsivity of CPD is larger under same low bias condition, but the two responsivities tend to be the same when the reverse bias increases to a value high enough. The exciting function of upgrading UV responsivity and degrading VIS counterpart simultaneously is realized by the novel GSPD, which could be a stimulating performance breakthrough for UV photodiode based on silicon crystal. It is for sure that new UV photodiodes based on silicon crystal with much better performance could be designed and realized under the guidance of our novel device configuration in the foreseeable future.

## References

[1] Yu A G. Semiconductor Near-Ultraviolet Photoelectronics. *Semiconductor Science and Technology*, 1999, **14**:41-60.

[2] Jones A R. Flame Failure Detection and Modern Boilers. *J Phys E: Sci Instr*, 1988, **21**:921-928.

[3] Pauchard A, Popovic R S. Ultraviolet Flame Detector. *Proceeding of the* 1998 *Microsystem Symposium*. Delft: Delft (NL) Press, 1998. 101-110.

[4] Diffey B L. *Ultraviolet Radiation in Medicine*. Bristol: Adam Hilger Inc, 1982. 23-25.

[5] Ganelina I E, Samoilova K A. *Mechanisms of Influence of UV Irradiated Blood on Organisms of Men and Animals*. Leningrad: Nauka (in Russian). 1986. 45-46.

[6] Parish G, Hansen M. AlGaN/GaN Solar-Blind Ultraviolet Photodiodes on SiC Substrate. *High Performance Devices*, 2000. *Proceedings*. 2000 *IEEE/Cornell Conference on* 7-9 *Aug*. New York: Cornell Press, 2000. 215-224.

[7] Poti B, Todaro M T. High Responsivity GaN-Based UV Detectors. *IEEE. Electronics Letters*, 2003, **39** (24): 1747-1749

[8] Razeghi M, Sandvik P. Lateral Epitaxial Overgrowth of GaN on Sapphire and Silicon Substrates for Ultraviolet Photodetector Applications. *Materials Science and Engineering*, 2000, **B74**:107-112.

[9] Vigue F, de Mierry P. High Detectivity ZnSe Based Schottky Barrier Photodetectors For Blue and Near Ultraviolet Spectral range. *IEEE Electron Device Letters*, 2000,**36**(4):352-354.

[10] Wen Rong-chang, Yean K F. The Hetero-Epitaxial SiCN/Si MSM Photodetector for High-Temperature Deep-UV Detecting Applications. *IEEE Electron Device Letters*, 2003, **24** (9):56.

[11] Korde R, Geist J. Quantum Efficiency Stability of Silicon Photodiodes. *Appl Opt*, 1987, **26**(24):52-84.

[12] Salib Mike, Liao Ling. Silicon Photonics. *Intel Technology Journal*, May 10, 2004,**8**(02):10-11.

[13] Thugngstrom G, Dubaric E. Processing of Silicon UV-photodetectors. *Nuclear Instruments and Methods in Physics Research A*, 2001, **460**:165-184.

[14] van Overstraeten R J. Transport Equations in Heavy Doped Silicon. *IEEE Trans Electron Device Letters*, 1973, **20**(3): 290.

[15] Chamberlain S G. Spectral Response Limitation Mechanisms. *IEEE Trans Electron Device Letters*, 1978, **25**(2):241.

[16] Robert Hull (Editor). *Properties of Crystalline Silicon*, London, UK:INSPEC IEE. 1999. 677.

[17] Vinod K K. Carrier Lifetimes and Recombination Generation Mechanisms in Semiconductor Device Physics. *Eur J Phys*, 2004, **25**:221-237.

[18] Schroder D K, Choi B D. Silicon Epitaxial Layer Recombination and Generation Lifetime Characterization. *IEEE Trans Electron Devices*, 2003, **50**(4):906-912.

[19] Schroder D K. Carrier Lifetimes in Silicon. *IEEE transactions on Electron Devices*, 1997, **44**(1):160-170.

□